Connecting the Automotive Bands of Present and Future With a Tag for Inharmonic Radar at 76–81/134–141 GHz

Tobias T. Braun, *Graduate Student Member, IEEE*, Jan Schöpfel, *Graduate Student Member, IEEE*, Christian Bredendiek, *Member, IEEE*, and Nils Pohl, *Senior Member, IEEE*

***Abstract*— Vulnerable road users like pedestrians, pedal-, and motorcyclists have accounted for an increasing proportion of traffic fatalities in the last 15 years. Simultaneously, harmonic radar systems have been implemented for applications where distinction between specific targets and surrounding clutter is required. However, the doubled frequencies conventionally used in harmonic radar systems are not licensed for automotive applications. Connecting the 76–81 GHz automotive band with the 134–141 GHz currently going through regulation instead necessitates what we propose to call inharmonic radar. Therefore, an innovative frequency modulation instead of doubling is required. This modulation is achieved and presented in this work with an active tag based on a novel 1.75 times fractional frequency multiplier. It successfully implements the required frequency conversion upward of –53 dBm of input power with undesired spectral components suppressed by more than 20 dB.**

***Index Terms*— Automotive, clutter suppression, *D*-band, frequency-modulated continuous wave (FMCW), harmonic, inharmonic, millimeter-wave (mm-wave), radar, SiGe, tag, vulnerable road users, *W*-band.**

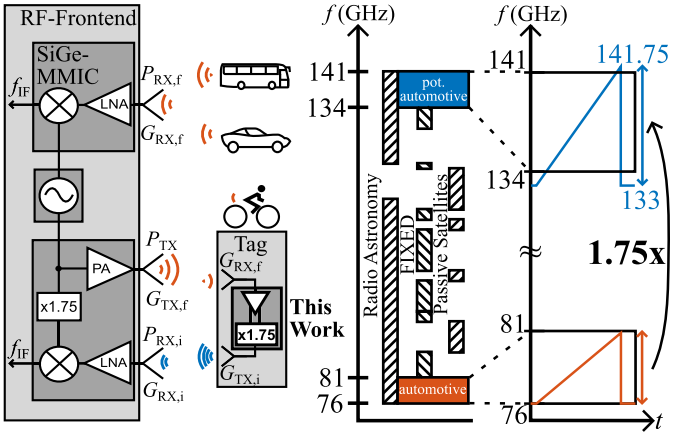

Fig. 1. Block diagram of the targeted inharmonic radar application. Utilizing the potential future automotive band from 134 to 141 GHz as the clutter-free receive channel is proposed for spectral compliance. This requires a tag based on novel 1.75 times frequency multiplication, which is presented in this work.

I. Introduction

AUTOMOTIVE radar sensors have become an integral part of the sensor technology integrated into today's cars. The main aim is increased traffic safety for people inside and surrounding the vehicle. However, according to the National Highway Traffic Safety Administration (NHTSA), the proportion of fatalities assigned to the group of outside vehicles, consisting of motor- and pedal cyclists, pedestrians, and other nonoccupants, has increased by 70% since 1996 [1]. This includes the highest number of fatal bicycle accidents in 2021 since data collection of the fatality analysis reporting system (FARS) started in 1975 [2]. Accordingly, the safety of vulnerable road users with a small radar cross section (RCS) should be of growing concern.

Therefore, we have presented a harmonic radar system in previous research [3], [4], [5]. It allows for detecting vulnerable road users like pedal cyclists in a separate, clutter-free receive channel. To distinguish them from the stronger linear reflections of their surroundings, they are equipped with an active tag. By multiplying the frequency of the received ramps by a factor N inside of this tag, they are, in theory, the only targets appearing when downconverting with this multiplied ramp at the radar system. The previous work is in line with other harmonic radar systems also based on $N = 2$ [6], [7], [8], [9], [10], [11], [12], [13], [14]. Advantageously, frequency doubling is easily realizable even at millimeter-wave (mm-wave) frequencies by Gilbert-cells or push-pull-doublers [15]. Medical applications, as presented in [16], can utilize that approach directly, thanks to the location of the ISM bands at 61/122 GHz [17]. In our case, the harmonic frequencies from 152 to 162 GHz are not licensed for automotive applications. They instead are part of a larger frequency band ranging from 151.5 to 164 GHz currently considered for 6G [18], [19].

Instead, a new automotive band around 140 GHz is currently being discussed [20]. Emerging as a firm favorite is the frequency band ranging from 134 to 141 GHz, which has already enticed the design of transceivers addressing this potential application [21], [22]. Among the advantages expected from this new band is an increased bandwidth

Manuscript received 30 October 2023; revised 22 December 2023; accepted 28 January 2024. Date of publication 16 February 2024; date of current version 10 April 2024. This work was supported in part by the German Federal Ministry of Education and Research (BMBF) partly in the course of the 6GEM research hub under Grant 16KISK037 and in part by the Research Project VERANO. *(Corresponding author: Tobias T. Braun.)*

Tobias T. Braun and Jan Schöpfel are with the Institute of Integrated Systems, Ruhr University Bochum, 44801 Bochum, Germany (e-mail: tobias.t.braun@rub.de).

Christian Bredendiek is with the Institute for High Frequency Physics and Radar Techniques FHR, 53343 Wachtberg, Germany.

Nils Pohl is with the Institute of Integrated Systems, Ruhr University Bochum, 44801 Bochum, Germany, and also with the Institute for High Frequency Physics and Radar Techniques FHR, 53343 Wachtberg, Germany.

Color versions of one or more figures in this letter are available at https://doi.org/10.1109/LMWT.2024.3362385.

Digital Object Identifier 10.1109/LMWT.2024.3362385

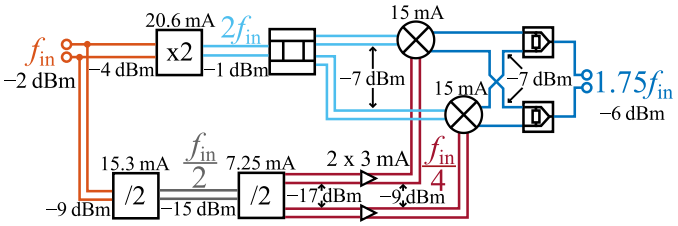

Fig. 2. Block diagram of the proposed frequency multiplier. To generate $f_{out} = 1.75 \cdot f_{in}$, a quarter of the input frequency is subtracted from its doubled signal with an SSB-mixer. Additionally, the simulated differential large signal power into every component after interstage matching losses is given, as well as their individual current consumption from a 3.3-V supply.

of 7 GHz. It can be utilized to improve range resolution and interference avoidance, while angular resolution benefits from the reduced wavelength [23], [24]. Apart from those advantages for fundamental radar systems, this potential new band represents a possibility for the tag-based detection of vulnerable road users to adhere to the regulations of the future frequency spectrum.

Instead of harmonic, the relation between the two bands necessitates what we propose to call inharmonic radar, in harmony with music theory [25], [26], therefore, requiring an innovative frequency conversion approach. It is the topic of this article and achieved with a tag based on a novel $N = 1.75$ frequency multiplier. The resulting harmonic seventh of the automotive band from 76 to 81 GHz equals 133–141.75 GHz, thus covering the potential new band from 134 to 141 GHz completely, as illustrated in Fig. 1 alongside the targeted application.

II. Monolithic Microwave Integrated Circuit

The developed realization of this uniquely required frequency conversion is illustrated in Fig. 2. It is based on the frequency doubler from the harmonic tag presented in [4], complemented by a /4-divider. Subsequently, a single-sideband (SSB) mixer is used. It consists of two individual mixer cells multiplying its 90° phase-shifted input signals in the time domain. Adding the mixers' outputs as

$$s_{out}(t) = \cos\left(\frac{\omega_{in}}{4}t\right) \cdot \sin(2\omega_{in}t) - \sin\left(\frac{\omega_{in}}{4}t\right) \cdot \cos(2\omega_{in}t) = \sin(1.75\omega_{in}t) \quad (1)$$

exclusively results in the desired multiplication factor.

To come as close to this perfect sine wave at the desired frequency as possible, the phase-shifted, or IQ, signals are required. A scaled version of the integrated hybrid coupler presented in [27] provides those for the doubled frequency. A layout view is depicted in Fig. 3(a). Port 1 acts as the input, while Port 4 is isolated with a 100-Ω resistor. The outputs at the other two ports are designed to offer the required phase shift with a low-amplitude imbalance.

A /4-divider based on two subsequent /2-stages provides the other required frequency. Each stage consists of a fedback D-Flip-Flop comprised of two latches. Both are realized in emitter-coupled logic (ECL) with inductive shunt peaking exclusively in the first stage [28]. The schematic of the /4-divider and specifically the second stage is illustrated in

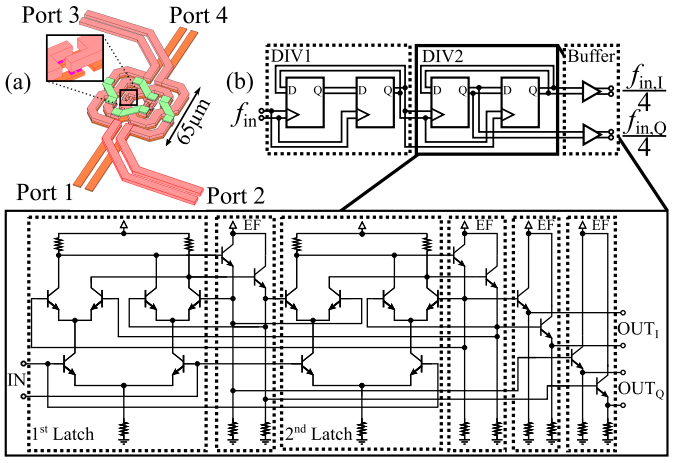

Fig. 3. Components responsible for the generation of the IQ signals: (a) scaled version of the Lange coupler presented in [27] for the doubled frequency and (b) the intrinsic 90° phase shift between the two latches of the second divider is used for the IQ generation of the quartered input frequency.

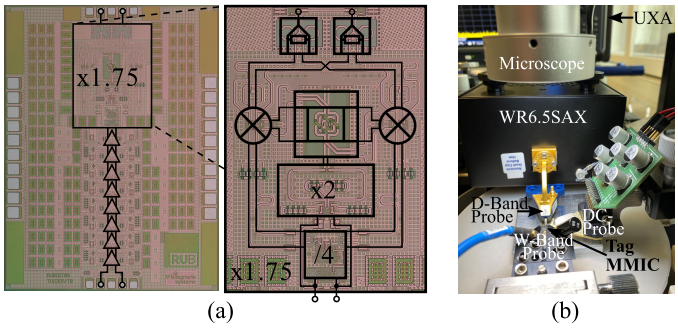

Fig. 4. (a) Micrograph of the realized tag with a close-up of the novel frequency multiplier. (b) Photograph of the measurement setup.

Fig. 3(b). Utilizing the output of both latches provides the required IQ signals [29]. A buffer amplifies each before acting as one input of the corresponding mixer, both of which consist of the same Gilbert-cell with an inductive load, similar to [30].

These individual components come together on the realized tag, of which a micrograph is presented in Fig. 4(a), with a close-up of the 1.75 frequency multiplier. As to not introduce additional phase and amplitude imbalance, a significant focus was placed on the symmetry of the layout. Therefore, the input is matched to the frequency doubler and /4-divider simultaneously, which are arranged in series. Thus, only one orthogonal crossing of the doubler's input and the divider's output is required. The coupler's output and mixer's input are designed point symmetrically for identical transmission line lengths. An amplifier chain is located in front of the multiplier, as presented in [4]. It is essential as the way to the tag primarily limits the maximum range by defining an R^{-2} proportionality when achieving P_{sat} instead of R^{-6} if not [4], [7]. Additionally, the sensitivity curve of the introduced divider means that for input powers that are too low, the output power at the desired frequency will equal zero when the divider stops working. The amplifier chain will stop that from happening for as high of a range between the tag and the radar as possible.

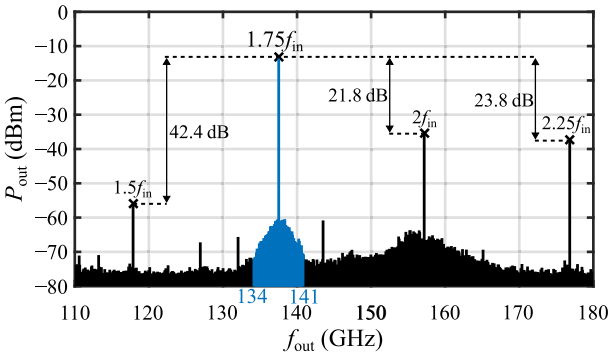

Fig. 5. Output spectrum measured single-endedly for a desired frequency of 137.5 GHz. The signal of 1.75 f_{in} is clearly the strongest, with good spectral purity. In the final application, it will be further improved by the symmetrical load, bond wires included in the output matching, and filtered by the antenna.

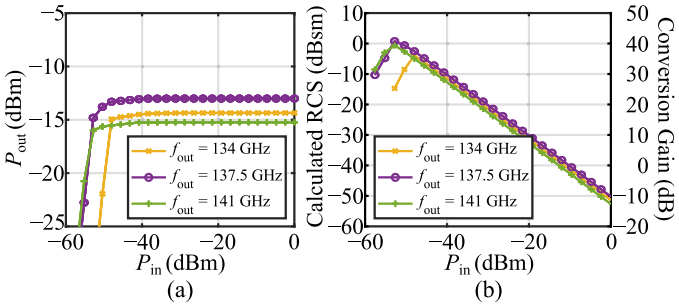

Fig. 6. (a) Compression curve of the inharmonic tag measured on-chip at the minimum, center, and maximum frequencies of the desired band. The tag sends out its P_{sat} down to −49 to −53 dBm of the input power, depending on the frequency. (b) Resulting in a maximum conversion gain of 40 dB and calculated RCS of 0 dBsm with assumed 12 dBi input and output antennas.

In total, the monolithic microwave integrated circuit (MMIC's) dimensions are 1448 × 1964 μm^2 with an active area of 500 × 1790 μm^2. It consumes a current of 120 mA from a 3.3-V power supply.

III. Measurement Results

Subsequently, the tag is measured on a probe station to validate its functionality. Therefore, the input signal is provided by a PSG by Keysight Technologies and multiplied via a frequency sextupler to reach the automotive band. The output spectrum is measured single-endedly with Keysight's UXA with a waveguide probe attached to a WR6.5SAX from VDI, as shown in Fig. 4(b). The resulting spectrum for a desired center frequency of the 134–141 GHz band of 137.5 GHz is shown in Fig. 5. Clearly, the desired frequency at 1.75 f_{in} represents the strongest signal. The undesired sideband at 2.25 f_{in} offers a sideband suppression of 23.8 dB. Additionally, the measurement shows leakage at 2 f_{in} with an amplitude 21.8 dB lower than the desired frequency. While those results are promising, as shown, they are expected to improve further in the final application. The 2 f_{in} leakage is significantly reduced when applying a symmetrical load in simulations. Additionally, the matching network at the output was designed to include bond wires, with which the sideband suppression is increased. Finally, the tag PCB will include an antenna whose resonance bandwidth further filters the output signal.

As the frequency conversion with high spectral purity is verified successfully, the dependency of the input power is subsequently investigated. It was varied by a programmable attenuator behind the W-band sextupler. The obtained results for the minimum, center, and maximum frequencies of the desired band are presented in Fig. 6. For an input power $P_{3\,dB}$ of −49 to −53 dBm, the tag sends out upward of 3 dB less than its saturated output power. This P_{sat} reaches up to −12 dBm single-endedly. The maximum conversion gain of 40 dB results in an equivalent RCS of 0 dBsm for antennas with 12 dBi at input and output, when calculated as shown in [3]. Inside an inharmonic radar at f_{out} =137.5 GHz, saturation occurs, if

$$P_{RX,tag} = P_{TX} + G_{TX,f} + G_{RX,f} - \mathrm{FSPL_f} > -53\,\mathrm{dBm} \quad (2)$$

with the radar system's and tag's antenna gain and the free-space path loss at the fundamental frequency as $G_{TX,f}$, $G_{TX,f}$, and $\mathrm{FSPL_f}$, respectively. Subsequently, the power received at the radar system $P_{RX,i}$ can be calculated as

$$P_{RX,i} = P_{sat} + G_{TX,i} + G_{RX,i} - \mathrm{FSPL_i} \quad (3)$$

with the system's and tag's inharmonic antenna gain $G_{RX,i}$ and $G_{TX,i}$, and inharmonic free-space path loss $\mathrm{FSPL_i}$, respectively. Due to the sophisticated multiplication factor with its additional components, the presented tag exhibits a higher current consumption than the state of the art in Table I. However, the parameters for the link budget compare very favorably. Therefore, it should allow for tens of meters of detectable range in the targeted radar application, while introducing spectral compliance for automotive.

TABLE I
State-of-the-Art Frequency Converting RF Tags

Ref.	Year	f_{in} (GHz)	N	P_{sat} (dBm)	P_{3dB} (dBm)	Range (m)	P_{DC} (mW)	Spectral Compliance
This	2023	79	1.75	−12$^+$	−53	-	396	Yes*
[4]	2022	79	2	−18	−57	80	89.1	No
[6]	2020	61	2	−4	−37	23	132	Yes$^\#$
[8]	2022	14	2	−20	−23	46	0	No

* Band at 134–141 GHz currently going through regulation
\# Not regulated for automotive applications
\+ Differential ouput should provide 3 dB higher P_{sat}

IV. Conclusion

In this article, we presented an active tag for automotive applications. It successfully connects the current automotive band at 76–81 GHz with the likely future band at 134–141 GHz. Therefore, an implementation of a 1.75 frequency multiplier was proposed and realized. For a desired center output frequency of 137.5 GHz, a suppression of undesired sidebands and the LO signal of at least 21.8 dB were measured single-endedly. The tag sends out its P_{sat} upward of −53 dBm, which should allow for tens of meters of clutter-free detectable range inside an inharmonic radar.

Acknowledgment

The authors would like to thank Infineon Technologies AG for fabricating the chips.

REFERENCES

[1] *Overview of Motor Vehicle Crashes in 2021*, Stewart, Nat. Highway Traffic Safety Admin., Washington, DC, USA, Apr. 2023.

[2] National Center for Statistics and Analysis, *Traffic Safety Facts 2019: A Compilation of Motor Vehicle Crash Data*, Nat. Highway Traffic Safety Admin., Washington, DC, USA, Aug. 2021.

[3] T. T. Braun, J. Schöpfel, C. Schweer, and N. Pohl, "A harmonic automotive radar for bicycle detection with RFID tags at 79/158 GHz," in *IEEE MTT-S Int. Microw. Symp. Dig.*, Jun. 2022, pp. 526–529.

[4] T. T. Braun, J. Schöpfel, P. Kwiatkowski, C. Schweer, K. Aufinger, and N. Pohl, "Expanding the capabilities of automotive radar for bicycle detection with harmonic RFID tags at 79/158 GHz," *IEEE Trans. Microw. Theory Techn.*, vol. 71, no. 1, pp. 320–329, Jan. 2023.

[5] T. T. Braun, J. Schöpfel, and N. Pohl, "Detecting vulnerable road users utilizing the harmonic RCS of active tags at 79/158 GHz," in *Proc. IEEE Radar Conf.*, May 2023, pp. 1–5.

[6] S. Hansen, C. Bredendiek, and N. Pohl, "Active reflector tag for millimeter wave harmonic radar at 61/122 GHz ISM band based on 130 nm-BiCMOS SiGe: C technology," in *IEEE MTT-S Int. Microw. Symp. Dig.*, Aug. 2020, pp. 611–614.

[7] S. Hansen, C. Bredendiek, G. Briese, and N. Pohl, "A compact harmonic radar system with active tags at 61/122 GHz ISM band in SiGe BiCMOS for precise localization," *IEEE Trans. Microw. Theory Techn.*, vol. 69, no. 1, pp. 906–915, Jan. 2021.

[8] C. Lynch, A. O. Adeyeye, A. Eid, J. G. D. Hester, and M. M. Tentzeris, "5G/mm-wave fully-passive dual Rotman lens-based harmonic mmID for long range microlocalization over wide angular ranges," *IEEE Trans. Microw. Theory Techn.*, vol. 71, no. 1, pp. 330–338, Jan. 2023.

[9] J. Shefer and R. J. Klensch, "Harmonic radar helps autos avoid collisions," *IEEE Spectr.*, vol. S-10, no. 5, pp. 38–45, May 1973.

[10] B. G. Colpitts and G. Boiteau, "Harmonic radar transceiver design: Miniature tags for insect tracking," *IEEE Trans. Antennas Propag.*, vol. 52, no. 11, pp. 2825–2832, Nov. 2004.

[11] D. Psychoudakis, W. Moulder, C.-C. Chen, H. Zhu, and J. L. Volakis, "A portable low-power harmonic radar system and conformal tag for insect tracking," *IEEE Antennas Wireless Propag. Lett.*, vol. 7, pp. 444–447, 2008.

[12] H. Heuermann, T. Harzheim, and M. Mühmel, "A maritime harmonic radar search and rescue system using passive and active tags," in *Proc. 17th Eur. Radar Conf. (EuRAD)*, Jan. 2021, pp. 73–76.

[13] A. Lavrenko, "Effects of bistatic operation in harmonic radar," in *Proc. 19th Eur. Radar Conf.*, 2022, pp. 1–4.

[14] J. Alam, M. Khaliel, A. El-Awamry, F. Zheng, K. Solbach, and T. Kaiser, "A mathematical framework, simulation, and measurement of harmonic identification systems," *IEEE Access*, vol. 11, pp. 71811–71822, 2023.

[15] T. Jaeschke, C. Bredendiek, S. Küppers, and N. Pohl, "High-precision D-band FMCW-radar sensor based on a wideband SiGe-transceiver MMIC," *IEEE Trans. Microw. Theory Techn.*, vol. 62, no. 12, pp. 3582–3597, Dec. 2014.

[16] A. Orth et al., "A compact harmonic radar system at 61/122 GHz ISM band for physiological joint angle estimation," in *Proc. 19th Eur. Radar Conf. (EuRAD)*, Sep. 2022, pp. 1–4.

[17] *FCC Online Table of Frequency Allocations*, FCC, Washington, DC, USA, Jul. 2022.

[18] *Radio Frequency Channel/Block Arrangements for Fixed Service Systems Operating in the Bands 130–134 GHz 141–148.5 GHz 151.5–164 GHz and 167–174.8 GHz*, Electron. Commun. Committee (ECC), Copenhagen, Denmark, Apr. 2018.

[19] M. J. Marcus, "6G spectrum policy issues above 100 GHz," *IEEE Wireless Commun.*, vol. 28, no. 6, pp. 7–8, Dec. 2021.

[20] A. Filippi, V. Martinez, and M. Vlot, "Spectrum for automotive radar in the 140 GHz band in Europe," in *Proc. 19th Eur. Radar Conf. (EuRAD)*, Sep. 2022, pp. 1–4.

[21] B. Sene, D. Reiter, H. Knapp, H. Li, T. Braun, and N. Pohl, "An automotive D-band FMCW radar sensor based on a SiGe-transceiver MMIC," *IEEE Microw. Wireless Compon. Lett.*, vol. 32, no. 3, pp. 194–197, Mar. 2022.

[22] I. Kraus, H. Knapp, D. Reiter, and N. Pohl, "A compact 140-GHz radar MMIC with I/Q downconverter in SiGe BiCMOS technology," in *IEEE MTT-S Int. Microw. Symp. Dig.*, Jun. 2023, pp. 509–512.

[23] L. L. Tovar Torres, T. Grebner, and C. Waldschmidt, "Automotive radar interference avoidance strategies for complex traffic scenarios," in *Proc. IEEE Radar Conf.*, May 2023, pp. 1–6.

[24] M. Köhler, J. Hasch, H. L. Blöcher, and L.-P. Schmidt, "Feasibility of automotive radar at frequencies beyond 100 GHz," *Int. J. Microw. Wireless Technol.*, vol. 5, no. 1, pp. 49–54, Feb. 2013.

[25] R. W. Young, "Inharmonicity of plain wire piano strings," *J. Acoust. Soc. Amer.*, vol. 24, p. 455, Jul. 1952.

[26] A. P. Klapuri, "Multiple fundamental frequency estimation based on harmonicity and spectral smoothness," *IEEE Trans. Speech Audio Process.*, vol. 11, no. 6, pp. 804–816, Nov. 2003.

[27] J. Schoepfel, T. T. Braun, S. Kueppers, K. Aufinger, and N. Pohl, "A fully differential hybrid coupler for automotive radar applications," in *Proc. 17th Eur. Microw. Integr. Circuits Conf. (EuMIC)*, Sep. 2022, pp. 107–110.

[28] C. Bredendiek, K. Aufinger, and N. Pohl, "Full waveguide E- and W-band fundamental VCOs in SiGe: C technology for next generation FMCW radars sensors," in *Proc. 14th Eur. Microw. Integr. Circuits Conf. (EuMIC)*, Sep. 2019, pp. 148–151.

[29] S. Henzler and S. Koeppe, "Design and application of power optimized high-speed CMOS frequency dividers," *IEEE Trans. Very Large Scale Integr. (VLSI) Syst.*, vol. 16, no. 11, pp. 1513–1520, Nov. 2008.

[30] J. Schoepfel, S. Kueppers, K. Aufinger, and N. Pohl, "A SiGe transceiver chipset for automotive radar applications using wideband modulation sequences," *Int. J. Microw. Wireless Technol.*, vol. 11, no. 7, pp. 676–685, Sep. 2019.